Sustainable Energy, Grids and Networks 26 (2021) 100437

Contents lists available at ScienceDirect

Sustainable Energy, Grids and Networks

journal homepage: www.elsevier.com/locate/segan

OPF solution for a real Czech urban meshed distribution network using a genetic algorithm

Ladislav Foltyn [a], Jan Vysocký [b], Giuseppe Prettico [c,*], Michal Běloch [a], Pavel Praks [a], Gianluca Fulli [c]

[a] IT4Innovations, VŠB—Technical University of Ostrava, 708 00 Ostrava, Czech Republic
[b] ENET Centre, VŠB—Technical University of Ostrava, 708 00 Ostrava, Czech Republic
[c] European Commission, Joint Research Centre (JRC), Ispra (VA), Italy

ARTICLE INFO

Article history:
Received 21 July 2020
Received in revised form 10 December 2020
Accepted 15 January 2021
Available online 23 January 2021

Keywords:
Genetic algorithms
Optimisation
Electrical distribution network
Pandapower
Active power demand
Transformer taps control

ABSTRACT

Electrical distribution networks are facing an energy transition which entails an increase of decentralised renewable energy sources and electric vehicles. The resulting temporal and spatial uncertainty in the generation/load patterns challenges the operations of an infrastructure not designed for such a transition. In this situation, Optimal Power Flow methods can play a key role in identifying system weak points and supporting efficient management of the electrical networks, including the distribution level. In this work, to support distribution system operators' decision-making process, we aim at attaining a quasi-optimal solution in the shortest time possible in an electrical network experiencing a large growth of distributed energy sources. We propose an optimisation method based on a modified version of a genetic algorithm and the Python pandapower package. The method is tested on a model of a real urban meshed network of a large Czech city. The optimisation method minimises the total operating costs of the distribution network by controlling selected network components and parameters, namely the transformer tap changers and the active power demand at consumption nodes. The results of our method are compared with the exact solution showing that a close-to-optimal solution of the observed problem can be reached in a relatively short time.

1. Introduction

Conceived several decades ago to supply electrical power generated by few large power plants to end consumers, power systems (mainly transmission and distribution systems) have recently undergone radical changes. Firstly, the whole sector was made more efficient. The electricity business deregulation and unbundling policies put in place in the 1990s established more competitive markets (in particular at the generation and retail level). Later, increasing concerns over climate change pushed for an enormous increase of electrical power production from renewable sources (mainly wind and photovoltaic modules). As a result, the current production of electrical power has become more decentralised, with a general tendency to generate electrical power closer to where it is consumed [1]. Additionally, power consumers have started to produce and consume their own electrical power, metamorphosing themselves into prosumers. Despite of the multitude of benefits these changes have had, and continue to have on air quality and on the climate as a whole, the operation of electrical distribution networks has become considerably more challenging. At any given time in an electrical power system, the balance between the power supply and power demand must be preserved. The stability of other electrical parameters (e.g. voltage and frequency) must be ensured as well. Constant values for these parameters are required both by the operating rules and the power consumers. The consumers' requirements have been becoming more and more stringent in recent years [2].

To enable the distribution system operators (DSOs) to operate safely, reliably, and to supply consumers with an electrical power satisfying all power quality requirements, distribution networks are being equipped with measuring devices for the active and reactive power, for voltage and current magnitudes and angles, etc. These components are equipped with software which sets individual network devices to make the distribution system (DS) operate optimally.

The first DS optimisation algorithms were developed in the 1950s [3,4]. These algorithms sought the optimal topology of reconfigurable radial distribution networks with the goal of minimising total active power losses in the network. In 1968, the

* Corresponding author.
E-mail addresses: ladislav.foltyn@vsb.cz (L. Foltyn), jan.vysocky@vsb.cz (J. Vysocký), Giuseppe.PRETTICO@ec.europa.eu (G. Prettico), michal.beloch@vsb.cz (M. Běloch), pavel.praks@vsb.cz (P. Praks), Gianluca.FULLI@ec.europa.eu (G. Fulli).

https://doi.org/10.1016/j.segan.2021.100437

standard problem of DS operation with minimum costs called Optimal Power Flow (OPF) was formulated [5]. In the following years, this standard optimisation problem was studied by many researchers who came up with many formulations of it, and many approaches to its solution.

In recent years, OPF research has been divided into several branches, with each branch highlighting a different issue. Currently, most of the attention is devoted to OPF problems that consider powering the observed power system with power plants using renewable energy sources of intermittent nature, and efficient use of battery energy storage. There is also a growing interest in the application of demand-side management in power flow regulation. Recent trends and aims of power system optimisation research are presented in [6]. In [7] a comprehensive survey of recent optimisation techniques used to solve OPF problems is presented. Traditional methods often suffer from local minimum issues, so alternative optimisation techniques are needed which are categorised based on their inspirations, such as nature-swarm-inspired methods, human-inspired algorithms, evolutionary-inspired algorithms, physics-inspired, and artificial neural networks (ANN). It is important to note that many research activities today focus on reducing the gap between academic studies and the real problems faced by power system operators. Researchers are also looking for new formulations of risk-based AC OPF problems under uncertainty that consider flexible security criteria. A trending current topic is the development of new methods for decomposing the AC OPF problem into smaller problems that are more easily solvable than the original problem and which can be solved in parallel during one time period. It should also be noted that significant progress has recently been made in developing OPF problem solvers that are based on local optimisers derived from general-purpose optimisers. Despite their optimal performance, these local optimisers sometimes fail to converge, especially for highly constrained feasible problems. More in-depth insights regarding the current trends in OPF research can also be found in [8,9].

As mentioned, in the emerging transition, DSOs are required to act more and more frequently in real-time. In [10], the authors develop a cascading outage probabilistic risk assessment based on the decomposition of the analysis in two levels corresponding to two stages of a cascading failure: the slow cascade and the fast cascade. The slow cascade is caused by the contingency occurrence in a power system with N-1 security criteria where the occurrence of just one contingency cannot cause a fast collapse of the power system. However, it can trigger a thermal transient, significantly increasing the occurrence of additional contingencies. The fast cascade follows the slow cascade: it is triggered when another contingency occurs and there is still electrical instability caused by the first contingency. For the electrical instability in the power system, authors consider voltage, frequency, and transient angular instability, and static violation of overcurrent limits. The voltage instability is detected through the non-convergence of power flow equations, the frequency instability through the steady-state frequency deviation, and the transient angular instability through the simulation of a simplified dynamic model of the power system during several seconds.

Apart from managing outages, the existence of local markets where prosumers can make bids/offers to exchange electrical power is becoming increasingly possible, which makes real-time operation of the DS necessary. To cope with these tasks, DSOs will need to be able to perform OPF analyses in the shortest possible time. However, this is not trivial even for networks of reduced size.

In this paper, we present a method for solving an AC OPF problem, optimising the operation of a real electrical distribution network (powering a part of a Czech city). Our approach, based on the genetic algorithm (GA), allows us to find an optimal solution effectively and efficiently. To ensure this fact, the GA was compared to the particle swarm optimisation (PSO) algorithm, which is also commonly used to solve OPF problems [6]. In the development process of our optimisation method, we relied on the approaches presented in [11–13]. Our optimisation method controls the transformers' on-load tap changers and the power load demands of consumption nodes to find global optima that satisfy operation constraints of a portion of the distribution network of a large city in the Czech Republic. The constraints include, among others, a voltage magnitude range and lines' and transformers' maximum current loading. More in depth, our optimisation method:

- is tuned to effectively and efficiently optimise the operation of highly-meshed distribution networks;
- allows us to evaluate the computational model with the discontinuities and conditioned penalties;
- is easily traceable in each step of its iterative cycle, so that it is always possible to tune the algorithm for individual cases to reach its best performance.

The remainder of the paper is organised as follows. Section 2 presents the optimisation problem, Section 3 describes the real Czech urban meshed network used as case study. Section 4 discusses our modified version of the GA method as a solver of this problem. Section 5 provides some numerical experiments with our GA method and benchmarks its results with the (brute force) exact solution. Section 6 concludes the work with a summary and a discussion of future potential activities.

2. Description of the problem

The OPF aim is to optimise the steady-state performance of the power system expressed through a given objective function while satisfying a set of equality and inequality constraints at the same time. A general formulation of the OPF is presented in [6]. In our case, the distribution system's operation costs are minimised while all solution constraints are maintained within their limits. The formulation of the problem is presented in the following sections. The internal structure of this OPF problem uses per-unit quantities. Apparent powers of individual network elements are related to a reference apparent power equal to 1 MVA, whereas magnitudes of individual node voltages are related to the nominal voltage of the network, which includes the given node.

2.1. Objective function

In the distribution network, there are n_{cn} power consumption nodes, while the power consumption of some of them can be controlled by the DSO. These nodes are called controlled power consumption nodes and their number is n_{cc}. The network also includes n_{pll} low-voltage (LV) power lines and n_{tr} distribution transformers. The set of all nodes with power consumption control is divided into two subsets: a set of first-grade consumption nodes and a set of second-grade consumption nodes. First-grade consumption nodes refer to those nodes where flexible consumers are connected. These nodes are the most suitable for dynamic power consumption control and to offer demand response services to DSOs. It is in the interest of the DSO that the maximum part of negative regulation power (i.e. reduction of power consumption) is provided by appliances connected to this set of consumption nodes. The remaining nodes with power consumption control are included in the set of second-grade consumption nodes. Appliances connected to these consumption nodes also allow their instantaneous power input to be controlled

by the DSO, but their involvement in the final process of regulating power flows in the distribution network is not suitable for physical, economic, and social reasons. The preferential use of power input reduction control in the first-grade consumption nodes during the power flow regulation process is ensured by different values of the power consumption reduction price for the first-grade consumption nodes and for the second-grade consumption nodes in the objective function.

Our OPF model minimises the following objective (cost) function C:

$$C = \sum_{i=1}^{n_{cc}} (C_{cc\_i} + C_{Pcc\_i}) + \sum_{j=1}^{n_{pll}} C_{\Delta P pll\_j} + \sum_{m=1}^{n_{tr}} C_{\Delta P tr\_m} + \sum_{p=1}^{n_{cn}} P_{Vl\_p} + P_{Qo} \tag{1}$$

where C_{cc_i} is the cost related to a change of power consumption of the ith power consumer and C_{Pcc_i} is the cost related to the magnitude of this change of power consumption, $i = 1, 2, \ldots, n_{cc}$; $C_{\Delta Ppll\_j}$ is the cost related to the magnitude of an active power loss of the jth LV power line, $j = 1, 2, \ldots, n_{pll}$; $C_{\Delta Ptr\_m}$ is the cost related to the magnitude of an active power loss of the mth distribution transformer, $m = 1, 2, \ldots, n_{tr}$; P_{Vl_p} is the penalty related to the voltage-limit exceeding in the pth network consumption node (i.e., a node which is connected to a power consumer), $p = 1, 2, \ldots, n_{cn}$; and P_{Qo} is the penalty related to the reactive power overload of the powering higher-level distribution system. Note that the last two members of the objective function were created via a transformation of the two soft solution constraints presented below.

The individual costs observed by the objective function are defined as:

$$C_{cc\_i} = \begin{cases} C_{fcc}\,,\ i \in N_{cn1} \\ C_{scc}\,,\ i \in N_{cn2} \end{cases} \tag{2}$$

$$C_{Pcc\_i} = \begin{cases} c_{fcc} \cdot \Delta P_i\,,\ i \in N_{cn1} \\ c_{scc} \cdot \Delta P_i\,,\ i \in N_{cn2} \end{cases} \tag{3}$$

$$C_{\Delta Ppll\_j} = c_{\Delta P} \cdot \Delta P_{pll\_j}\,,\ j \in \{1, \ldots, n_{pll}\} \tag{4}$$

$$C_{\Delta Ptr\_m} = c_{\Delta P} \cdot \Delta P_{tr\_m}\,,\ m \in \{1, \ldots, n_{tr}\} \tag{5}$$

$$P_{Vl\_p} = p_{Vl} \cdot \left|V_p - V_{sl}\right|^2\,,\ p \in \{1, \ldots, n_{cn}\} \tag{6}$$

$$P_{Qo} = \begin{cases} p_{Qo} \cdot |Q_e|^3\,,\ Q_e < 0 \\ 0,\ Q_e \geq 0 \end{cases} \tag{7}$$

where the meaning of the used symbols is as follows:

- C_{fcc} denotes the cost related to a change of power consumption at a first-grade controlled consumption node;
- C_{scc} is the cost related to a change of power consumption at a second-grade controlled consumption node;
- N_{cn1} is the set of first-grade controlled-consumption nodes;
- N_{cn2} is the set of second-grade controlled-consumption nodes;
- c_{fcc} is the cost per unit (in €/MW) related to the magnitude of a change of power consumption at a first-grade controlled consumption node;
- c_{scc} is the cost per unit (in €/MW) related to the magnitude of a change of power consumption at a second-grade controlled consumption node;
- ΔP_i is the magnitude of a change of power consumption at the ith consumption node, $i = 1, 2, \ldots, n_{cc}$;
- $c_{\Delta P}$ is the cost per unit (in €/MW) related to the magnitude of an active power loss of a network element;
- ΔP_{pll_j} is the magnitude of an active power loss in the jth LV power line, $j = 1, 2, \ldots, n_{pll}$;
- ΔP_{tr_m} is the magnitude of an active power loss in the mth distribution transformer, $m = 1, 2, \ldots, n_{tr}$;
- p_{Vl} is the penalty per unit (in €/V) related to the voltage-limit exceeding at a consumption node;
- V_p is the magnitude of voltage at the pth consumption node, $p = 1, 2, \ldots, n_{cn}$;
- V_{sl} is the soft limit of a voltage phasors magnitude, where

$$V_{sl} = \begin{cases} V_{max\_sl}\,, & V_p > V_{max\_sl} \\ V_{min\_sl}\,, & V_p < V_{min\_sl} \\ V_p\,, & V_{min\_sl} \leq V_p \leq V_{max\_sl} \end{cases}, \quad p \in \{1, \ldots, n_{cn}\} \tag{8}$$

- V_{min_sl} and V_{max_sl} are the minimum and maximum values of the soft limit of a voltage phasors magnitude;
- p_{Qo} is the penalty per unit (in €/Mvar) related to magnitude of a reactive power overload to the powering higher-level distribution system;
- Q_e is the magnitude of a reactive power flowing to or from the distribution network through the slack node e.

2.2. Constraints

The OPF problem's solution space is constrained by equality and inequality constraints. Some of them are hard, i.e. they set certain conditions on the variables that must be satisfied, while some are soft, meaning they do not need to be strictly satisfied, but their exceeding is penalised in the objective function.

2.2.1. Hard constraints

Inequality constraints describe the maximum current loading of the power lines and transformers (current loading of the transformers' primary winding), the minimum and maximum admitted values of voltage's magnitudes in individual LV network nodes, and the minimum and maximum admitted values of individual local distribution transformers' taps. They are expressed as follows:

$$I_{pl\_i} \leq I_{pl\_max\_i}\,, \quad i \in N_{pl} \tag{9}$$

$$I_{tr\_i} \leq I_{tr\_max\_i}\,, \quad i \in N_{tr} \tag{10}$$

$$V_{min\_fl} \leq V_i \leq V_{max\_fl}\,, \quad i \in N_{nl} \tag{11}$$

$$t_{min\_i} \leq t_i \leq t_{max\_i}\,, \quad i \in N_{tr} \tag{12}$$

- where I_{pl_i} is the current flowing through the ith power line;
- $I_{pl\_max\_i}$ is the maximum current loading of the ith power line;
- N_{pl} is the set of local power lines' indices;
- I_{tr_i} is the current flowing through the primary winding of the ith distribution transformer;
- $I_{tr\_max\_i}$ is the maximum current loading of the primary winding of the ith distribution transformer;
- N_{tr} is the set of local distribution transformers' indices;
- V_i is the magnitude of voltage at the ith LV network node;
- V_{min_fl} and V_{max_fl} are the minimum and maximum admitted values of the voltage's magnitude at the individual LV network nodes;
- N_{nl} is the set of LV-network nodes' indices;
- t_i is the tap settings of the ith distribution transformer;
- t_{min_i} and t_{max_i} denote the minimum and maximum value of tap settings of the ith distribution transformer.

2.2.2. Soft constraints

Although soft constraints do not restrain the problem's feasible space, they have a large impact on the specific final solution. In our OPF problem, one soft constraint is observed. It describes the limits of the voltage's magnitude at the individual LV network nodes:

$$V_{min\_sl} \leq V_i \leq V_{max\_sl}\,, \quad i \in N_{nl} \tag{13}$$

Table 1
Constant values of the objective function.

C_{fcc}	C_{scc}	c_{fcc}	c_{scc}	$c_{\Delta P}$	p_{Vl}	p_{Qo}
$15 \cdot 10^{-4}$ €	$3 \cdot 10^{-3}$ €	0.6 €/MW	0.9 €/MW	1.0428 €/MW	$1 \cdot 10^{-5}$ €/V	0.02 €/kvar

Table 2
Constants used in the inequality constraints.

$I_{pl\_max\_i}$	$I_{tr\_max\_i}$	V_{min_fl}	V_{max_fl}	t_{min_i}	t_{max_i}	V_{min_sl}	V_{max_sl}
1	1	0.85	1.1	−2	2	0.95	1.02

As mentioned above, we consider soft constraints in the OPF problem as a penalty added to the objective function. The penalty considering the soft constraint (13) is formulated as:

$$\sum_{p=1}^{n_{cn}} P_{Vl\_p} \tag{14}$$

With respect to the considered constants in the objective function, Table 1 summarises their values:

The values of the constants in Table 1 are derived from the price of electricity on the Czech wholesale electricity market (pxe market) in the following way: we use the predicted price of purchased electricity for a peak load consumption in 2021[1] (on the pxe market, the peak-load time is set for Monday through Friday, 8 a.m. to 8 p.m., the base-load time is every day from 0 a.m. to 12 p.m.). The peak-load electricity price per MWh is divided by 60 min. This is done because we assume that the steady frequency of the optimisation system's control actions will correspond to one action per minute. Consequently, it is assumed that the energy loss in the network during this one-minute time interval is equal to dP · 1 min, where dP is the total active power loss.

This cost model is based on the pxe peak-load electricity price traded on 1.10.2019 (i.e. 62.57 €/MWh). As a result, the price per MW · minute is 1.0428 €:

$$c_{\Delta P} = \frac{62.57€/\text{MWh}}{60\,\text{min}} = 1.0428\,€/\text{MW}$$

The values of other price coefficients used in formulas (1) to (7) were set with regard to the value of $c_{\Delta P}$ and to the optimisation goals, which are based on the requirements of the DSO. During individual test runs, the ratios between the individual members of the objective function and the total value of the objective function were observed. Based on these observed values, the individual price coefficients were adjusted so that the values of all the ratios were approximately the same.

In the inequality constraints we use the individual constants shown in Table 2:

The values $I_{pl\_max\_i}$ and $I_{tr\_max\_i}$ are set to 100%, which means that each network element can be loaded for a long time (or permanently) only by a current whose magnitude is not bigger than 100% of its maximum current-carrying capacity (otherwise the element would be overloaded and its maximum allowable temperature would be exceeded). The individual local power line sections are constructed using different types of power carrying cables and each type has its own value for maximum current-carrying capacity, determined by its producer. The maximum current-carrying capacity value for individual cable types is defined in Amperes. Likewise, the transformer producer determines the value of the maximum current-carrying capacity for each transformer. The electrical network model used in the optimisation method presented in this paper contains a specific maximum current-carrying capacity value for each power line section and each transformer. As mentioned above, the mathematical system used within the local AC power flow problem is based on per-unit values. In order to assess whether a given steady-state of the distribution network does not exceed the overcurrent limit for any of the network elements, it is necessary to convert the per-unit values of currents flowing through individual network elements to actual values expressed in Amperes. These values in Amperes are then compared to the defined overcurrent limits for individual network elements.

The value of V_{min_fl} is set to 0.85 because the undervoltage limit set by the DS's operating regulations is 85% of the nominal voltage of the LV network. Similarly, the value of V_{max_fl} is set to 1.1 because the overvoltage limit set by the DS's operating regulations is 110% of the nominal voltage of the LV network. Because the DSO's goal is to achieve the highest possible power quality, it also sets soft limits for the value of the voltage magnitude, i.e. V_{min_sl} and V_{max_sl}. These soft limits determine the area of high-quality electrical energy in terms of voltage magnitude, and their distance from 1 (i.e. the per-unit nominal-voltage value) is much less than the distance of the limits defining undervoltage and overvoltage from 1. The values of t_{min_i} and t_{max_i} are described in the following section.

3. Description of the test model

The method's optimisation performance and efficiency were tested on the model of a portion of a real Czech urban mesh LV distribution network. The distribution network model consists of 46 LV nodes (the nominal line voltage of these LV nodes is 0.4 kV) and 6 medium-voltage (MV) nodes (the nominal line voltage of these MV nodes is 22 kV).

The 6 MV nodes operate as slack nodes in the model (these 6 slack nodes are then aggregated into one slack node, *e*, in the model). The magnitude and phase of the voltage phasors in these nodes are constant and are permanently equal to 1 and 0°, respectively (this set of 6 slack nodes can also be described as one slack node and 5 PQ nodes, which are connected with the slack node by network elements, the impedance of which is equal to zero, and the active and reactive power consumption of which are equal to zero as well). These 6 nodes provide power balance within the network model.

The reason why all nodes of the MV side of all transformers in this distribution network are connected to one common slack node are the following: Measurements performed in the six local MV/LV substations showed that from the point of view of all these six substations, the differences in the absolute value and phase of the voltage phasors on the MV side are negligible. Very small impedances connecting individual MV nodes of individual local MV/LV transformers caused by small lengths and large cross-section areas of local MV cables are the main reason for these very small differences of the voltage phasors. Based on these findings, we have decided to connect all six local MV nodes into one node in order to reduce the size of the admittance matrix of the network mathematical model by five rows and five columns. This significantly reduces the computational complexity of the local AC-power-flow solution without reducing the accuracy of this model.

Moving down, 6 LV nodes serve as LV network supply nodes. Each of these 6 LV nodes is connected to one of the 6 slack buses using a distribution transformer. The remaining 40 LV nodes are

[1] https://www.pxe.cz/Products/Detail.aspx?isin=FCZPLY211231#KL.

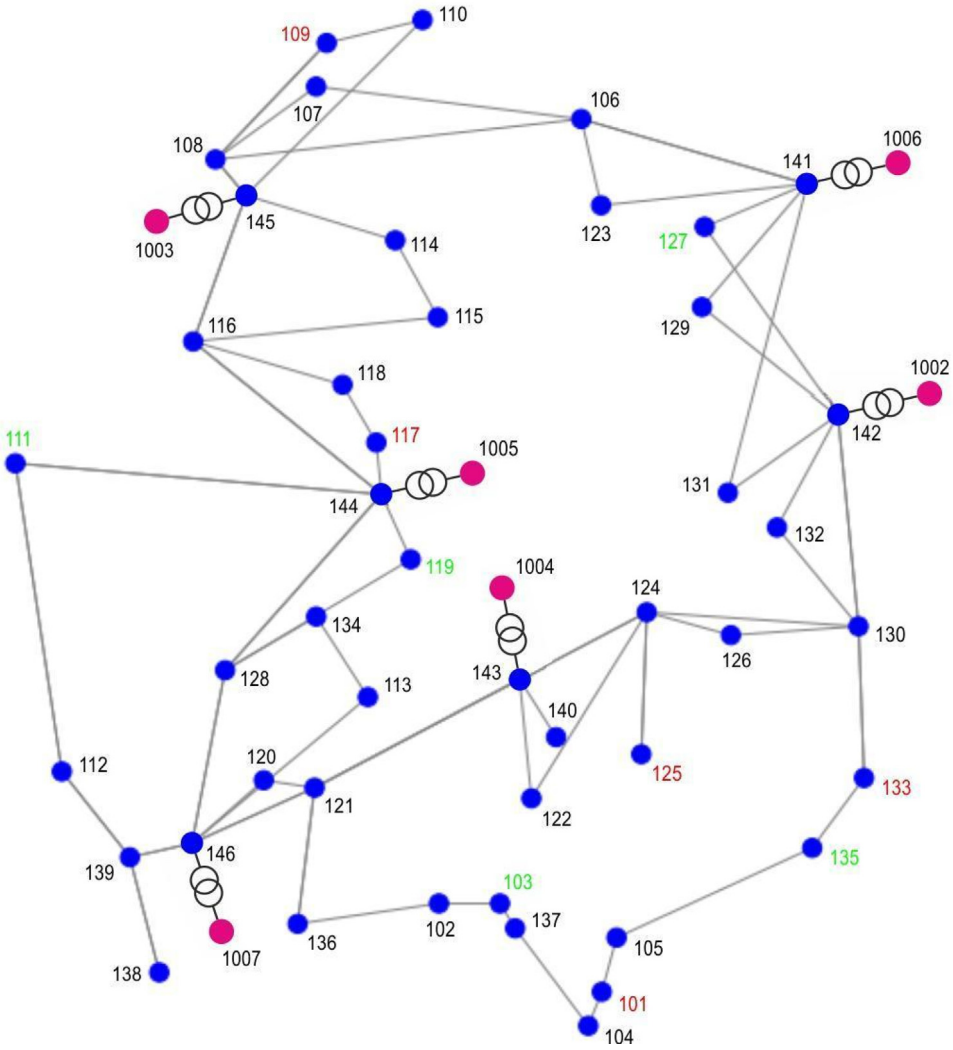

Fig. 1. Topology of the analysed Czech urban meshed distribution network. (For interpretation of the references to colour in this figure legend, the reader is referred to the web version of this article.)

consumption nodes, each connected to a power load. As mentioned above, the magnitude of the active power consumption of some consumption nodes is controlled by our optimisation method (that is, by the DSO in practice). Of these consumption nodes, 5 are classified as first-grade controlled-consumption nodes and 5 as second-grade controlled-consumption nodes. In summary, there are 10 loads connected to the distribution network, for which the active power consumption can be controlled by our optimisation method. Until the optimisation method activates the control of a node's power consumption, the active and reactive power consumed in this node is determined by the standard needs of the local consumer. These standard values for both classes of controlled-consumption nodes represent 100% of the amount of power consumption and are listed in Tables 3 and 4. If the optimisation method activates the control of the power consumption in a given node, then the amount of active power consumed in that node drops to 85% of the standard amount of local active power consumption. However, the amount of reactive power consumed in this node remains 100% of the standard amount of local reactive power consumption.

In the apartment buildings connected to the controlled consumption nodes, there are electric heaters installed. These appliances can be controlled remotely by the DSO. Electrical appliances of this kind are very suitable tool for power balancing inside the distribution network. Every unit has a quite large power input, and its remote control can serve this scope. During the cold part of the year, it operates for several hours every day, and during its operation, the value of its power input is constant in time. Because the optimisation method optimally controls the distribution network in real-time, it needs to know how much electrical power is currently consumed in the network. Thus, the current balance of active and reactive power in individual consumption nodes of this network is continuously observed in real-time using modern measuring devices, KMB SMC 144.[2] The DSO gets the information about the currently-accessible controllable power consumption also from this power data.

Tables 3, 4, and 5 describe all LV-network nodes using their indices and the amount of active and reactive power they consume.

As there is only one type of distribution transformer installed in the distribution network, the values of individuals parameters of all local transformers are the same. The nominal turns ratio of these transformers is 22 kV/0.4 kV, their nominal apparent power is 400 kVA, their percentual short-circuit voltage is 6% and their percentual open-circuit current is 0.1075%. On the transformers' primary side (i.e. middle-voltage side), there are on-load tap changers (OLTC) installed. An OLTC allows changing of the

[2] http://www.kmb.cz/index.php/en/power-monitor-data-logger/smc-144.

transformer's turns ratio when the transformer is loaded. Each local OLTC has 5 taps. Rated tap is the centre one, so the taps range from −2 to 2 (the t_{min_i} is equal to −2 and the t_{max_i} is equal to 2). After switching from tap X to tap X + 1, the voltage on the transformer's secondary side increases by 2.5% of the secondary side's nominal voltage.

One capacitor is connected to each consumption node of the LV network. These capacitors operate here as local reactive power sources, producing a constant reactive power of 6.5 kvar. Usual Czech city distribution networks are not equipped with any capacitors and until recently, there were no capacitors in the network presented in this paper. However then, the local DSO decided to install the capacitors into this network as part of the process of increasing the network operation efficiency. This process is part of the test project and this network was the only one where the DSO installed the capacitors. The specific nominal value of the reactive power of the individual local capacitors, equal to 6.5-kvar, was chosen on the basis of historical data measured in this network. Historical data have shown that the total reactive power consumption inside this network does not fall below 260 kvar for a long time. So, the DSO decided to cover this minimum total reactive power consumption by local production, while the total amount of reactive power was equally divided between all 40 consumption nodes, so the nominal reactive power of individual local capacitors is equal to 260 kvar/40 = 6.5 kvar.

Fig. 1 shows a scheme of the whole distribution network. The first grade controlled consumption nodes are marked with red coloured text, the second grade controlled consumption nodes are marked with green coloured text and the uncontrolled consumption nodes are marked with black coloured text. Fig. 1 also shows 6 MV nodes: these MV nodes are marked by indices 1002, 1003, 1004, 1005, 1006 and 1007.

Although it is common to see LV distribution networks supplying apartment buildings in housing estates in Czech cities using a meshed topology and being supplied through more than one MV/LV substation, the rate of mutual connections of individual network nodes and the number of MV/LV substations in the distribution network presented in the paper are unusual from the Czech electrical networks perspectives. The high spatial density of consumption nodes and high power consumption of these nodes (individual local consumption nodes represents apartment buildings) are the reason for the unusual characteristics of this network.

From the long-time view, the size of power consumption of individual apartments in apartment buildings connected to individual local consumption nodes is approximately the same. This distribution network supplies many apartment buildings. In each apartment building, there are many apartments and these apartments are connected to the network in such a way that approximately the same number of apartments is powered by each network phase. Based on these facts, there was an idea that at any time the power consumption in this distribution network is (approximately) equally distributed into individual distribution network phases. Consequently, at any time all three phase conductors of individual power-line sections in any part of the network are (approximately) equally loaded. Later, this idea was verified by measurements done in all local MV/LV substations. The validity of this idea made it possible to describe this distribution network using a 1-phase model. The computational complexity of the 1-phase AC power flow solution is much lower than the 3-phase AC power flow solution. Since most of the computational time of the optimisation algorithm presented in this paper is consumed by the AC power flow solution calculation, the usage of the less complex 1-phase AC power flow solution leads to the much lower computational complexity of the whole optimisation algorithm.

3.1. Loads connected to the controlled-consumption nodes

Table 3
First-grade controlled-consumption nodes.

First-grade		
Node's index	P (kW)	Q (kvar)
101	50	5
109	100	10
117	90	3
125	220	15
133	100	13

Table 4
Second-grade controlled-consumption nodes.

Second-grade		
Node's index	P (kW)	Q (kvar)
103	70	2
111	140	6
119	110	8
127	110	7
135	130	3

3.2. Loads connected to the uncontrolled-consumption nodes

Table 5
Uncontrolled-consumption nodes.

Node's index	P (kW)	Q (kvar)	Node's index	P (kW)	Q (kvar)	Node's index	P (kW)	Q (kvar)
102	30	0.5	122	25	2	105	40	2
104	30	0.2	124	20	0.1	113	40	2
106	30	0.5	126	30	0.2	121	40	5
108	30	0.2	128	30	2	129	40	5
110	20	0.2	130	20	1	137	40	5
112	30	0.5	132	20	0.5	107	50	3
114	50	0.2	134	30	1	115	40	5
116	10	0.1	136	20	0.5	123	30	2
118	20	2	138	30	0.5	131	50	3
120	25	2	140	40	1	139	40	2

4. Genetic algorithm as an optimisation method

Genetic algorithms are described in good detail in [14,15]. A version of GA using the information of the weighted gradient in the mutation process is presented in [16,17]. Our modified version of the GA is based on the main idea of the crossover and mutation step.

Let

$$P = \left\{X_1^0; X_2^0; \ldots; X_n^0\right\}, n \in N \tag{15}$$

be a population of chromosomes, where X_i^k denotes the ith chromosome in the kth generation. Every chromosome consists of two genes: the first one codes the configuration of transformer taps, the second codes the percentages of active power demands at the controllable consumption nodes, as follows:

$$X_i^k = \left[\left(t_{i,1}^k; t_{i,2}^k; t_{i,3}^k; t_{i,4}^k; t_{i,5}^k; t_{i,6}^k\right); \left(l_{i,1}^k; l_{i,2}^k; l_{i,3}^k; l_{i,4}^k; l_{i,5}^k; l_{i,6}^k; l_{i,7}^k; l_{i,8}^k; l_{i,9}^k; l_{i,10}^k\right)\right].$$

. $t_{i,j}^k \in \{-2; -1; 0; 1; 2\}, j = 1, 2$ is the tap number of the jth transformer in the kth generation and $l_{i,j}^k \in \{0.85; 1.0\}$ is the percentage of active power demands at the jth controllable

consumption node in the kth generation. The value of 0.85 corresponds to the maximum 15% decrease of power demand permitted on controllable loads. These load values reasonably constrain the space of valid solution. In each generation of the GA, we verify whether the individual chromosome, i.e. combination of transformer taps and active power load demands, falls in a feasible domain D_V or not. The feasible domain is composed by those cases in which the conditions (9)–(11) are satisfied after one run of the Python pandapower's power flow function [18]. Based on this simple test, we divide the population set into valid chromosomes

$$I_V^k = \left\{X_j^k : X_j^k \in D_V; \forall j\right\} \tag{16}$$

and invalid chromosomes

$$I_F^k = \left\{X_j^k : X_j^k \notin D_V; \forall j\right\}. \tag{17}$$

Then we proceed to the next steps of the algorithm.

In the step of creating offspring (chromosomes of the next generation), we prefer chromosomes from the set of valid chromosomes I_V^k over those from the invalid set I_F^k. The main steps of our algorithm can be summarised as follows:

1. Select 10% of the population size from the best valid chromosomes I_V^k as elite chromosomes which automatically proceed to the next generation. As the fitness value, we consider the actual cost of the performed network configuration. If there are fewer valid chromosomes I_V^k (less than 10% of the population size), choose all valid chromosomes I_V^k as elite chromosomes.
2. Create up to $2 \cdot n_V^k$ offspring from the valid chromosomes by crossover and mutation, where n_V^k is the number of valid chromosomes in kth generation. If $n_V^k > n$, then $n_V^k = n$. Chromosomes that progress to the crossover step are chosen by the roulette method.
3. Create up to $n_F^k = n - \left(2 \cdot n_V^k\right)$ offspring from the invalid chromosomes by crossover and mutation. Chromosomes proceeding to the crossover step are chosen randomly.

The stop criterion of the GA is a given maximum number of generations (which is estimated after many rounds of the algorithm). Note that the crossover step is always performed in each generation, that is, the crossover step has a 100% probability to occur.

4.1. Selection of valid chromosomes

We use a roulette technique as the selection method to choose parent chromosomes from the set of valid chromosomes I_V^k. Since we are interested in finding the global minimum (in the ideal case), a function that normalises the fitness values into the range [0;1] is

$$r\left(f_i^k\right) = \frac{f_{max}^k - f_i^k}{f_{sum}}, \tag{18}$$

where f_i^k is the fitness value of ith valid chromosome in the kth iteration, f_{max}^k represents the maximum fitness value of valid chromosomes in kth iteration, and f_{sum} denotes a summation of all fitness values of valid chromosomes in the kth iteration. We present pseudocode of the selection method for better illustration; see Algorithm 1.

Input: Vector of fitness values in the k-th iteration $\underline{f}$

Output: Indices of two selected parent chromosomes

$f_{sum} = sum\left(\underline{f}\right)$;

$f_{max} = max\left(\underline{f}\right)$;

Generate two random values in the range [0; 1);

tmp = 0;

For i = 1 to N:

$r_i = \frac{f_{max}^k - f_i^k}{f_{sum}}$;

tmp = tmp + r_i;

If Random_value_1 <= tmp:

Save index i;

If Random_value_2 <= tmp:

Save index i;

If two index are saved:

break;

Return selected indices

Algorithm 1: Pseudocode of the roulette method.

4.2. Crossover

In the crossover step, children's genes are derived from parent's genes. A random index $i_R = rand(2, i_{end} - 1)$, from which the crossover begins, is generated. The symbol i_{end} represents the last index of the gene array. One child inherits from one parent the part of the gene up to a random index i_R. The rest of the chromosome is inherited from another parent to the end index i_{end}. The crossover step is performed for both genes separately.

4.3. Mutation

The mutation step allows us to randomly generate the new value from the given range in the gene notation. If we consider the gene of transformer taps, then the new value will be an integer in the range $[-2; 2]$. We also generate an index in which the mutation will proceed. Furthermore, we check whether the generated value is the same as the current one. If these two values are the same, we generate a new one that varies from the old one. Some recommendations about the mutation probability values can be found in [19]. We choose the highest probability (0.09) because we want to ensure that the GA will not get stuck in local optima, given the characteristics of our problem. Additionally, we mutate only one bit per chromosome. The mutation probability value of 9% is based on numerical experiments.

4.4. Parallel implementation

The main objective of the parallel implementation of the GA is to reduce the computational time of the Python pandapower's

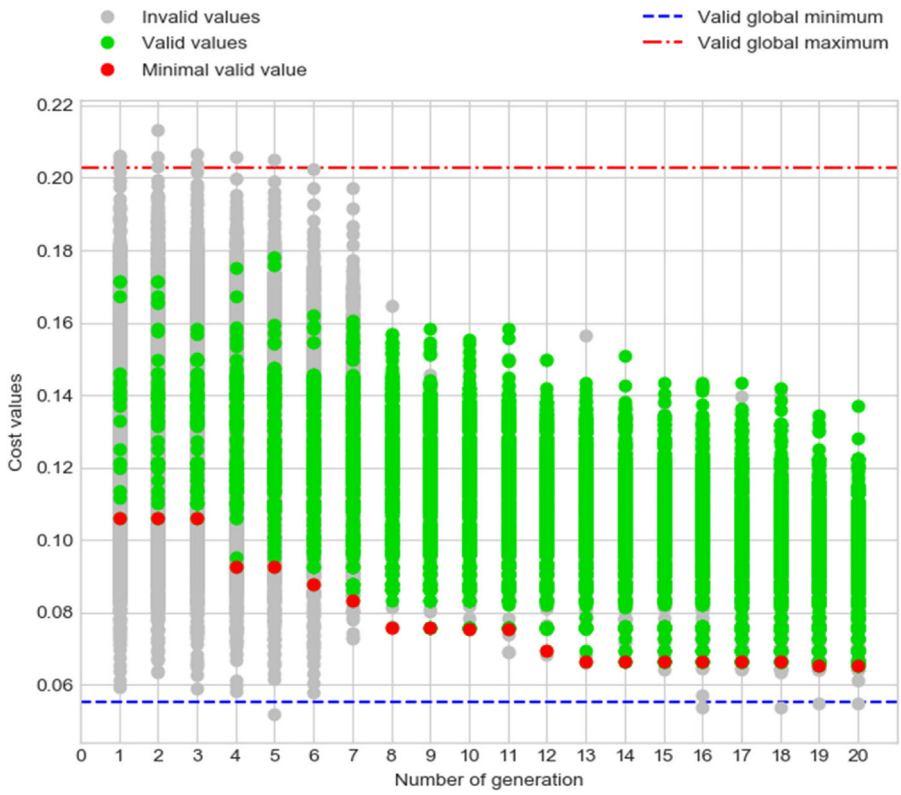

Fig. 2. Progress per generation of the single run of the GA. (For interpretation of the references to colour in this figure legend, the reader is referred to the web version of this article.)

Table 6
Parameters used in the GA.

Population size	Number of generations	Mutation probability	Number of elite chromosomes
2400	20	9%	240

Table 7
Resulting values of the exact solution.

Number of all possible combinations	Number of all valid combinations	Global valid minimum cost value	Global valid maximum cost value
16,000,000	135,639	0.05516	0.20267

power flow function that evaluates network variables. Steps such as the evaluation of the fitness function, crossover, and mutation are performed in parallel. The validation of chromosomes and the choice of the elite ones is instead done sequentially due to the fact that we need to assemble the array of all fitness values.

4.5. Modification

The core of the modification of GA lies in the way the sets of valid and invalid chromosomes are used within the algorithm. The chromosomes are not only created on the basis of crossover and mutation operator processes, but also by considering the validity of the results the chromosome gives. The chromosomes labelled as valid have a higher priority to make offspring than invalid ones. However, the invalid chromosomes are by no means forbidden. They are also used to make offspring, because combinations of two invalid chromosomes could result in a valid chromosome. The same can be true for a combination of a valid and invalid pair.

5. Numerical experiments

In the numerical experiments, we use the GA parameters described in Table 6. Note that the described parameters of the GA are all used in the analysis below. The resulting values of the exact solution are instead summarised in Table 7.

We can see from Table 7 that the brute force algorithm provides a wide range of valid solutions. The cost value based on 16 million possible combinations varies from 0.05516 € to 0.20267 €. However, we are interested in the combinations leading to the optimal solution, which provides the minimal valid cost. In the next subsections, we provide the results of our modified genetic algorithm, which are used for fast but accurate approximations of the optimal solution. We also perform a comparison of the GA to the PSO in the last subsection.

Numerical experiments were performed on an HP Spectre x360 Convertible 13-ap xxx, Intel(R) Core(TM) i7-8565U 1.80 GHz with 8 logical cores, 16 GB RAM and implemented in Python.

5.1. Single run analysis

We provide an analysis of one run of our modified GA observing its numerical behaviour, i.e. a monotonous descent of the objective function value to the global minimum. We analyse the cost function C given by Eq. (1). All fitness values from each generation of the GA algorithm are shown in Fig. 2. The red dash-dotted line marks the valid global maximum fitness value, while the blue dashed line denotes the valid global minimum fitness value i.e. the optimal (minimal) value of the cost function C, which is 0.05516; see Table 7. Grey dots are values corresponding to the invalid chromosomes, green dots represent values of valid chromosomes. Finally, the red dots highlight the current minimal

Table 8
Number of valid chromosomes in each generation of the GA.

gen	1.	2.	3.	4.	5.	6.	7.	8.	9.	10.
N	19	50	107	231	428	787	1440	2179	2187	2195
gen	11.	12.	13.	14.	15.	16.	17.	18.	19.	20.
N	2187	2165	2166	2176	2179	2199	2181	2171	2192	2200

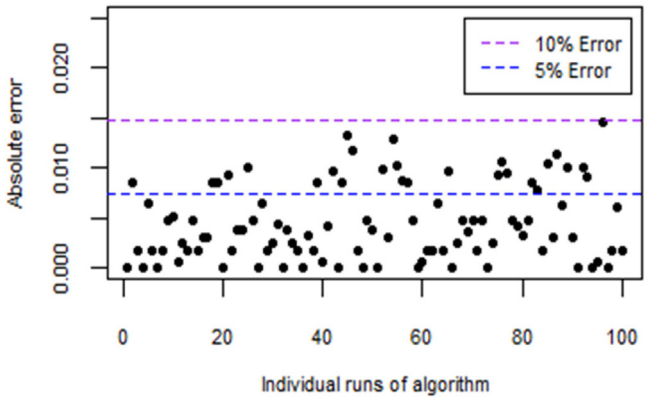

Fig. 3. Absolute errors of 100 GA runs in detail.

value, which tends to reach the valid global minimum. Fig. 2 shows that the valid global maximum fitness value can even be temporarily exceeded by invalid chromosomes.

The number of valid combinations in each generation is described in Table 8 respectively, where "gen" denotes the current generation and "N" represents the number of chromosomes in the current generation.

As we can see, one run of the GA evaluates 48,000 values (which imply in total 48,000 pandapower calls) for all 20 generations. Note that we choose 20 generations to be sure to obtain a stable solution. Another possibility is to use a tolerance limit to end the GA. It takes about 156 s to finish the calculations.

5.2. Multiple run analysis

To analyse the convergence of our GA we study its behaviour when launched multiple times. We ran the GA 100 times and observed its convergence. As a precision criterion, we consider the absolute error, which is defined as the difference between the resulting minimal value of the objective function found by our modified GA and the exact global minimum value. We choose the absolute error representation to demonstrate the distance of resulting values from the valid global minimum. Fig. 3 shows the minimal absolute error values of the GA.

The violet dashed horizontal line denotes the 10% of the maximum possible error, i.e. absolute error $y = 0.1 \cdot 0.148$, where 0.148 is the maximum possible error. Our aim was to reach at least 90% precision (i.e. limit the absolute error by 10%), and the purple line in Fig. 3 shows us that the aim was reached, as all dots representing the precision of GA runs are under this line. The blue dashed horizontal line is the cut-off for the 95% precision of our GA, i.e. it represents the absolute error $y = 0.05 \cdot 0.148$. Black dots mark minimal values from the individual runs of the GA.

All the minimal values satisfy our criterion for 90% precision, meaning all GA solutions are within the 10% error area. Remarkably, 73% of the values even satisfy the stricter criterion of 95% precision.

Table 9
Summarised statistical results.

Count	Minimum	Maximum	Average	Median	Std. deviation
135,639	0.000	0.148	0.082	0.083	0.025

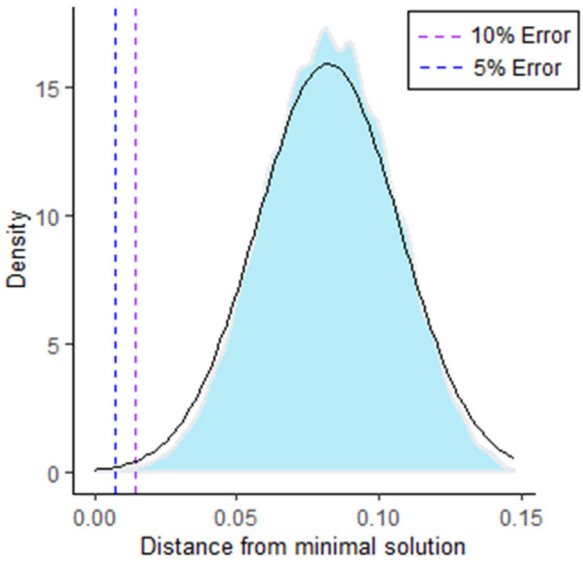

Fig. 4. Density function of the observed values.

5.3. Statistical analysis of the absolute error of multiple runs

In this section we analyse the absolute error of 100 GA runs. Let us remember that the optimal (minimal) value of the cost function C corresponds to 0.05516. Note that, as observed values are in the form of error values of all valid configurations of the network, the minimal error is $0.05516 - 0.05516 = 0$ and the maximal error is $0.20267 - 0.05516 = 0.14751$. A summary of the statistical results is shown in Table 9.

Fig. 4 shows the density function of the absolute error. Here, the black line represents the normal distribution using the parameters from Table 9. It can be seen that the computed error values loosely follow the normal distribution. This means that these values are mainly concentrated around the mean value of 0.082, and that the majority of computed values are in the $\pm 3\sigma$ area. The probability to randomly obtain a value within the 10% error threshold is 0.3%. Moreover, the probability to obtain $\leq 5\%$ absolute error is 0.1%. Fig. 5 shows a more detailed histogram of the best obtained results from 100 runs of the GA. Despite the low probabilities, the absolute error of the best GA values is within 10%. Moreover, we will also see that GA can reliably reach an approximation of the optimal solution.

Between the maximum absolute error and the minimum absolute error lie 135,637 different values. Within the range of 10% error, i.e. for 90% precision, there are 118 different values. These 118 values form only $118/135{,}637 \sim 8.7 \cdot 10^{-4} \sim 0.087\%$ of all valid values and only $7.375 \cdot 10^{-4}\%$ of the total 16 million combinations.

5.4. Sequential versus parallel computation

One run of sequential GA for 300 chromosomes in a generation takes approximately 72.78 s. Note that the GA computation time (mutation, crossover) is almost negligible. From analysis of the most expensive functions it emerges that, for each computation, pandapower creates a pandas structure (dataframe), which is subsequently transformed into a pypower structure suitable for

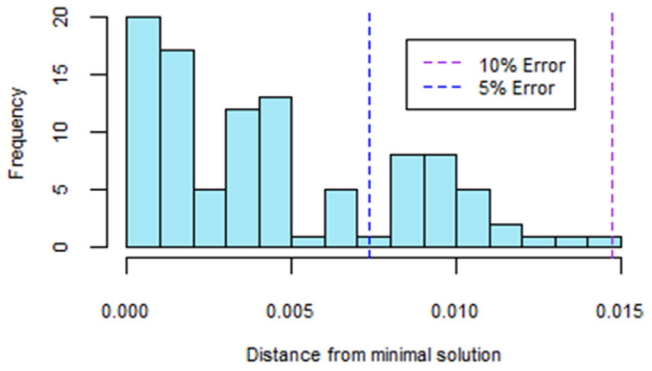

Fig. 5. A histogram detailing the best solutions.

Table 10
Results of PSO and GA.

N	PSO		GA	
	Error	Global index	Error	Global index
1.	0.06492	36.	0.06656	59.
2.	0.06605	49.	0.05581	2.
3.	0.06460	31.	0.05516	1.
4.	0.06367	26.	0.05682	3.
5.	0.05989	12.	0.05516	1.
6.	0.05989	12.	0.06330	24.
7.	0.06164	19.	0.05682	3.
8.	0.06367	26.	0.05581	2.
9.	0.05516	1.	0.05765	4.
10.	0.06367	26.	0.05989	12.

computation, and vice versa. A run of a parallel GA takes approximately 156 s with 300 chromosomes used per core. Even though the time increase is twice the run time of the sequential GA (due to the communication between processes), we are able to compute 8 times more pandapower simulations.

5.5. GA versus PSO

We choose the genetic algorithm due to its searching ability in the discrete space. From our point of view, the PSO algorithm is more suitable when the solution lies in the continuous space. We compared the GA with the PSO in a sequential mode for 300 elements per population with up to 20 iterations of the whole algorithm. We ran both algorithms 10 times. The results are shown in Table 10. The valid global minimum 0.05516 (see Table 7) has a global index equal to 1. This means that this value is the best one we can find, so we assigned it an ordered global index 1. The second best value has a global index equal to 2, etc. The average computational time of the GA is 48.17 s and the time of the PSO is 128.00 s, so the GA algorithm is 3 times faster than the PSO. We used the PSO algorithm from the Pyswarms package (https://pyswarms.readthedocs.io). We used the Pyswarms package (https://pyswarms.readthedocs.io) for the hyperparameter search of PSO parameters, and subsequently for the PSO optimisation.

6. Conclusions

Optimal Power Flow (OPF) methods can play a key role in ensuring efficient management and control of electrical distribution networks. In this paper, in line with current distribution system operators' needs, we have presented an OPF solving method which is applied to optimise the operation of a real Czech urban meshed electrical distribution network. Our method, based on a modified version of a Genetic Algorithm and on the use of the Python pandapower package, satisfies all given inequality constraints such as voltage magnitude range, and lines' and transformers' current loading, and converges to the solution very quickly. To demonstrate the robustness of the proposed algorithm, we performed several practical tests. By running 100 random instances of the problem, we were able to reach 90% precision of results for all the tests, meaning that all the results were close to the optimal solution with an absolute error of less than 10%. One run of our modified GA takes approximately 156 s in a parallel implementation on a standard laptop. It is obviously possible to reduce the computational time by using a more powerful workstation, but also by improving the GA code where the Python pandapower's power flow function is called. It is worth mentioning that our intuition to use both information from the feasible and the non-feasible domain in the GA is quite effective. In fact, we can reach the 90% precision criterion in our GA in only 20 generations of chromosomes. Practically speaking this means that we need to evaluate only 48,000 pandapower function calls out of 16 million possible combinations to achieve very high precision. Although other test cases can be implemented to verify the robustness of our modified GA, we can already state that our goal to make a GA-based algorithm that is robust and as fast as possible has been successfully achieved. Our next step is to be able to use it effectively and efficiently to optimise various types of electrical distribution networks. Because models of real distribution networks are not easy to obtain for security and confidential reasons, we will use the Distribution Network Model (DiNeMo) web-platform which reproduces realistic distribution network models of a given area of interest based on a small set of users' inputs [20]. In [21], a distribution network of a portion of the Varaždin city in Croatia has already been calculated through DiNeMo and validated with the DSO. This network model could be a good first candidate to further test the performance of our proposed GA-based method.

Declaration of competing interest

The authors declare that they have no known competing financial interests or personal relationships that could have appeared to influence the work reported in this paper.

Acknowledgements

This work was supported by The Ministry of Education, Youth and Sports, Czech Republic from the National Programme of Sustainability (NPS II) project "IT4Innovations excellence in science - LQ1602" and by The Ministry of Education, Youth and Sports, Czech Republic from the Large Infrastructures for Research, Experimental Development, and Innovations project "e-INFRA CZ – LM2018140". This work has been also partially supported by the Technology Agency of the Czech Republic under the projects "Optimization of the electrical distribution system operating parameters using artificial intelligence" TJ02000157 and "Energy System for Grids" TK02030039.

References

[1] I.E. Agency, World Energy Outlook 2018, International Energy Agency, 2018.
[2] G. Prettico, M.G. Flammini, N. Andreadou, S. Vitiello, G. Fulli, M. Masera, Distribution System Operators Observatory 2018 - Overview of the Electricity Distribution System in Europe, EUR 29615 EN, Publications Office of the European Union, Luxembourg, ISBN: 978-92-79-98738-0, 2019, http://dx.doi.org/10.2760/104777,JRC113926.
[3] L.K. Kirchmayer, G.H. McDaniel, Transmission losses and economic loading of power systems, Gen. Electr. Rev. 54 (10) (1951) 39–46.

[4] T.W. Sze, J.R. Garnett, J.F. Calvert, Some applications of a new approach to loss minimization in electrical utility systems, Trans. Amer. Inst. Electr. Eng. Part III: Power Appar. Syst. 77 (1958) 1577–1585, http://dx.doi.org/10.1109/aieepas.1958.4500206.
[5] H. Dommel, W. Tinney, Optimal power flow solutions, IEEE Trans. Power Appar. Syst. PAS-87 (1968) 1866–1876, http://dx.doi.org/10.1109/tpas.1968.292150.
[6] J. Vysocky, S. Misak, Review of trends and targets of complex systems for power system optimization, Energies 13 (2020) 1079, http://dx.doi.org/10.3390/en13051079.
[7] M. Ebeed, S. Kamel, F. Jurado, Optimal power flow using recent optimization techniques, Class. Recent Aspects Power Syst. Optim. (2018) 157–183, http://dx.doi.org/10.1016/b978-0-12-812441-3.00007-0.
[8] J.M. Capitanescu, P. Ramos, D. Panciatici, A.M. Kirschen, L. Marcolini, F. Platbrood, et al., State-of-the-art, challenges, and future trends in security constrained optimal power flow, Electr. Power Syst. Res. 81 (2011) 1731–1741, http://dx.doi.org/10.1016/j.epsr.2011.04.003.
[9] F. Capitanescu, Critical review of recent advances and further developments needed in AC optimal power flow, Electr. Power Syst. Res. 136 (2016) 57–68, http://dx.doi.org/10.1016/j.epsr.2016.02.008.
[10] P. Henneaux, P.-E. Labeau, J.-C. Maun, L. Haarla, A two-level probabilistic risk assessment of cascading outages, IEEE Trans. Power Syst. 31 (2016) 2393–2403, http://dx.doi.org/10.1109/tpwrs.2015.2439214.
[11] P. Sreejaya, R. Rejitha, Reactive power and voltage control in kerala grid and optimization of control variables using genetic algorithm, in: 2008 Joint International Conference on Power System Technology and IEEE Power India Conference, 2008, http://dx.doi.org/10.1109/icpst.2008.4745156.
[12] A.-M. Vaduva, C. Bulac, New evolutionary algorithm method for solving optimal reactive power dispatch problem, in: 2016 International Conference on Applied and Theoretical Electricity (ICATE), 2016, http://dx.doi.org/10.1109/icate.2016.7754626.
[13] S. Stankovic, L. Soder, Optimal power flow based on genetic algorithms and clustering techniques, in: 2018 Power Systems Computation Conference (PSCC), 2018, http://dx.doi.org/10.23919/pscc.2018.8442583.
[14] D. Whitley, A genetic algorithm tutorial, Statist. Comput. 4 (1994) http://dx.doi.org/10.1007/bf00175354.
[15] J.H. Holland, Adaptation in Natural and Artificial Systems: An Introductory Analysis with Applications to Biology, Control, and Artificial Intelligence, MIT press, 1992, http://dx.doi.org/10.7551/mitpress/1090.001.0001.
[16] J. Tang, D. Wang, A new genetic algorithm for nonlinear programming problems, in: Proceedings of the 36th IEEE Conference on Decision and Control, 1997, http://dx.doi.org/10.1109/cdc.1997.649813.
[17] S. Liu, Z. Hou, Weighted gradient direction based chaos optimization algorithm for nonlinear programming problem, in: Proceedings of the 4th World Congress on Intelligent Control and Automation (Cat. No.02EX527), 2002, http://dx.doi.org/10.1109/wcica.2002.1021388.
[18] L. Thurner, A. Scheidler, F. Schafer, J.-H. Menke, J. Dollichon, F. Meier, et al., Pandapower—An open-source python tool for convenient modeling, analysis, and optimization of electric power systems, IEEE Trans. Power Syst. 33 (2018) 6510–6521, http://dx.doi.org/10.1109/tpwrs.2018.2829021.
[19] R. Greenwell, J. Angus, M. Finck, Optimal mutation probability for genetic algorithms, Math. Comput. Model. 21 (1995) 1–11, http://dx.doi.org/10.1016/0895-7177(95)00035-z.
[20] Dinemo: JRC smart electricity systems and interoperability, dinemo | JRC smart electricity systems and interoperability, 2020, https://ses.jrc.ec.europa.eu/dinemo (accessed October 7, 2020).
[21] M. Grzanic, M. Flammini, G. Prettico, Distribution network model platform: A first case study, Energies 12 (2019) 4079, http://dx.doi.org/10.3390/en12214079.